The Journal of Experimental Biology 212, 2057-2064
Published by The Company of Biologists 2009
doi:10.1242/jeb.030692

Rhabdom constriction enhances filtering by the red screening pigment in the eye of the Eastern Pale Clouded yellow butterfly, *Colias erate* (Pieridae)

Kentaro Arikawa[1,*], Primoz Pirih[2] and Doekele G. Stavenga[2]

[1]Laboratory of Neuroethology, Sokendai-Hayama, Hayama Center for Advanced Studies, Hayama, Japan and [2]Department of Neurobiophysics, University of Groningen, Groningen, The Netherlands

*Author for correspondence (e-mail: arikawa@soken.ac.jp)

Accepted 1 April 2009

SUMMARY

Here we report the remarkable anatomy of the eye of the Eastern Pale Clouded yellow butterfly, *Colias erate*. An ommatidium of *C. erate* bears nine photoreceptors, R1–9, which together form a tiered and fused rhabdom. The distal tier of the rhabdom consists of the rhabdomeral microvilli of R1–4 photoreceptors, R5–8 photoreceptors contribute the proximal tier, and the R9 photoreceptor adds a few microvilli at the base. In transverse sections, four spots of red pigment surrounding the rhabdom are evident in the ventral region of the eye. The red pigment acts as a strong red filter for the proximal photoreceptors. The arrangement of the pigment spots distinguishes the ommatidia into three types: trapezoidal (type I), square (type II) and rectangular (type III). In all types of ommatidia, the distal and the proximal tiers of the rhabdom are divided by a strong constriction, clearly to enhance the filtering effect of the red pigment. The ommatidial heterogeneity can also be observed by optical measurements. The eye shine, resulting from tapetal reflections, peaks in type I ommatidia at 660 nm, and in type II and III ommatidia at 730 nm. The far-red-peaking eye shine indicates that *C. erate* has far-red-sensitive photoreceptors. Type I ommatidia fluoresce under violet excitation, implying the presence of a violet-absorbing pigment that acts as a short-wavelength filter.

Key words: insect vision, compound eyes, eye shine, spectral heterogeneity.

INTRODUCTION

When viewed with an epi-illumination microscope, butterfly eyes commonly exhibit colourful reflections, the so-called eye shine, whose colour varies between ommatidia (Bernard and Miller, 1970; Stavenga et al., 2001; Qiu et al., 2002; Stavenga, 2002). The reflections are due to a tapetum, created by a tracheole located in each ommatidium at the proximal end of the rhabdom. Incident light that has travelled through the rhabdom without having been absorbed reaches the tapetum, and there it is reflected by the tapetum back into the rhabdom. Part of the reflected light, after having travelled back through the rhabdom, leaves the eye and is visible as the eye shine. The different colours of the individual ommatidia indicate that the ommatidia have different spectral properties.

The spectral heterogeneity of ommatidia is very common in compound eyes (Ribi, 1978; Franceschini et al., 1981; Hardie, 1986; Arikawa and Stavenga, 1997; Briscoe, 2008). In the Small White butterfly, *Pieris rapae crucivora*, the heterogeneity is directly seen from the eye shine: the ommatidial reflections are pale red or deep red, with spectral peaks at 635 nm and 675 nm light, respectively (Qiu et al., 2002). This difference is attributed to different pigments surrounding the rhabdom. The 635 nm-reflecting ommatidia contain a pale-red pigment, and the 675 nm-reflecting ommatidia have a deep-red pigment. The pale-red and deep-red pigments act as spectral filters for the proximal photoreceptors, which in all ommatidia express a visual pigment absorbing maximally in the yellow–green, at 563 nm. The spectral sensitivities of the proximal photoreceptors thus are strongly modified, resulting in two classes of red receptor, with peak wavelengths at 620 and 640 nm, respectively (Qiu and Arikawa, 2003; Wakakuwa et al., 2004).

Interestingly, the spectral organisation of butterfly eyes largely differs between species (Bernard, 1979; Stavenga et al., 2001). For example, the papilionid *Papilio xuthus* has only one class of red receptor, whose sensitivity peaks at 600 nm (Matic, 1983; Arikawa et al., 1987; Arikawa et al., 1999b), and in the nymphalids *Sasakia charonda* and *Polygonia c-aureum* no red receptors have been found (Kinoshita et al., 1997). In order to understand the biological meaning of the species-specific eye organisation, it is important to distinguish the retinal properties common among species and those restricted to certain species. We therefore have surveyed several butterfly species to see how their ommatidial heterogeneity can be recognised through their eye shine (Stavenga et al., 2001). We encountered two peculiar pierid species, the yellow tip *Anthocharis scolymus*, which completely lacks eye shine due to the absence of the tapetal mirror (Takemura et al., 2007), and the Eastern Pale Clouded yellow *Colias erate*, which under white light epi-illumination exhibits a bright-red eye shine only in the dorsal eye region.

How have such variable visual systems evolved in insects? With this specific question in mind, we have investigated the anatomy of the eye of *C. erate*. *Colias erate* is an open grassland species occurring widely in Asia. The adults are rapid flyers that live in open grassland and frequently, but not exclusively, feed on red flowers (Tanaka, 1991). We found in *C. erate* that tapetal reflections do exist in all ommatidia including those in the ventral eye region. The majority of ventral ommatidia have a peak reflectance at a wavelength above 700 nm, due to a strongly absorbing red pigment. Based on extensive anatomical work and optical studies of the tapetal reflections, we identified three distinct types of ommatidia in the ventral eye region. The rhabdoms in all ommatidial types appear to have a strongly constricted region between the distal and proximal tiers. The constriction clearly has the effect of enhancing the filtering effect of the red perirhabdomal pigment.

MATERIALS AND METHODS

Animals

We used reared adults of the Eastern Pale Clouded yellow butterfly, *Colias erate* Esper. We collected females around the Sokendai Hayama campus, Kanagawa, Japan, and let them lay eggs on clover. We fed the hatched larvae with fresh leaves of their food plant (red clover *Trifolium pratense*) at 25°C under a light regime of 14 h light:10 h dark.

Anatomy

For electron microscopy, isolated eyes were prefixed in 2% paraformaldehyde and 2% glutaraldehyde in 0.1 mol l^{-1} sodium cacodylate buffer (CB, pH 7.3) for 30 min at 20–25°C. After a brief wash with 0.1 mol l^{-1} CB, the eyes were postfixed in 2% osmium tetroxide in 0.1 mol l^{-1} CB for 2 h at 20–25°C. Following dehydration with a graded series of acetone and infiltration with propylene oxide, eyes were embedded in Quetol 812 (Nisshin EM, Tokyo, Japan). Ultrathin sections, cut with a diamond knife, were stained with uranyl acetate and lead citrate, and observed in a transmission electron microscope (H7650, Hitachi, Tokyo, Japan). For light microscopy, the prefixed eyes were dehydrated and embedded in Quetol 812 without being postfixed with osmium tetroxide. The tissues were cut into 5 μm sections and observed with a light microscope (BX60, Olympus, Tokyo, Japan).

To correlate the ommatidial fluorescence with the tapetal reflection and the pigment around the rhabdom, we first photographed the fluorescence of an intact eye under 420 nm excitation from a large number of ommatidia using a modified epi-illumination telemicroscopic optical setup (Stavenga, 2002) equipped with an objective lens of large numerical aperture and long working distance (Olympus MPLFLN20, NA 0.45, WD 6.6 mm). We then photographed the tapetal reflection with the same setup, applying epi-illumination at wavelengths of 660 nm and 730 nm using interference filters. The eyes were subsequently processed for light microscopic histology as described above.

Using a series of electron micrographs obtained from a single eye, we quantified the pigment position and the rhabdom area. We counted the number of pigment granules per ommatidium in photoreceptors R5–8. The rhabdom areas were measured using iTEM software (Soft Imaging System, Riverside, CA, USA).

Imaging microspectrophotometry

For imaging microspectrophotometry (IMSP), we used a monochromatic camera (Roper Scientific, Tucson, AZ, USA). Illumination was provided by a computer-controlled monochromator (Delta Scan 4000, PTI, Birmingham, NJ, USA) with a 75 W xenon arc lamp. The monochromator output was coupled to a 1 mm diameter quartz light guide for IMSP of tapetal reflections, and to a 6 mm diameter liquid light guide for IMSP of histological sections. The fibre output, collimated with a quartz condenser, served as the light source.

For IMSP of the eye shine, we positioned an intact butterfly under the telemicroscope optical setup equipped with a Leitz LM32 NA 0.60 objective lens (Stavenga, 2002). The spectra of ommatidial reflections were recorded in five spectral runs from 550 nm to 850 nm in 5 nm steps. The five runs were as follows: two reflection runs (up and down the spectrum), a calibration run with a MgO-coated surface on the stage instead of a butterfly, and their two respective background measurements, which served to correct for lens reflections. The time interval between the monochromatic flashes, 5 s, was sufficiently long to avoid light adaptation.

For IMSP of histological sections, we investigated a plastic section of 5 μm thickness of non-osmicated eye tissue at a depth of 330 μm with a Zeiss Axiovert microscope equipped with an Olympus ×100 NA 1.30 immersion objective lens and illuminated the section with monochromatic light in the trans-illumination mode. We recorded the images in the wavelength range from 380 nm to 730 nm in 10 nm steps. We corrected the images for wavelength-dependent magnification (an inherent property of all microscope objectives tested) by affine transformation. We subsequently selected regions of interest around the clusters of red and black pigment granules and calculated the transmittance using clear areas of the section as the reference.

RESULTS

Eye regionalisation

The eye of *C. erate* consists of about 6500 ommatidia. The length of the dioptric apparatus (the cornea and crystalline cone) is about 100 μm. In the middle region of the eye, the length of the ommatidia, including the dioptric apparatus, is about 800 μm, while the ommatidia become shorter near the ventral and dorsal edges (Fig. 1A).

An ommatidium contains nine photoreceptors, R1–9, as in other butterflies. Photoreceptors R1–4 contribute the rhabdomeric microvilli to the distal tier of the rhabdom, whereas the rhabdom in the proximal tier consists of the rhabdomeres of the R5–8 photoreceptors. R9 adds a few microvilli at the base of the rhabdom. Proximal to the basement membrane, a trachea forms the tapetal mirror (Fig. 1B). The cell bodies of the R5–8 photoreceptors in the distal half of the retina have long and narrow extensions, which contain red pigment. The pigment can be clearly seen as red lines in unstained longitudinal sections of non-osmicated tissue only in the main, ventral eye region (Fig. 1C). The pigmentation is absent in the ommatidia in the dorsal one-third of the eye (Fig. 1A,D).

IMSP of the tapetal reflection

We observed the tapetal reflection of the eye of *C. erate* eye using a telemicroscopic optical setup (Stavenga, 2002). To measure the reflectance spectra by the IMSP method, we illuminated the eye with a series of monochromatic lights. Fig. 2A is a sample picture with 660 nm illumination. We analysed the reflectance spectra of 2300 ommatidia from five specimens and classified the ommatidia into three distinct types, dorsal-red (DR, peak reflectance at 670 nm), ventral-red (VR, 670 nm) and far-red (FR, 730 nm). Fig. 2B shows the median spectra for the three types (continuous curves) together with the interquartile spread of the spectra (lightly coloured areas).

Ommatidial fluorescence, tapetal reflection and pigment

Some of the butterfly species studied so far have fluorescing ommatidia (Arikawa et al., 1999a; Arikawa et al., 2005; Takemura et al., 2007). This also appears to be the case for *C. erate*. We found in the ventral region of the eye that the VR ommatidia (Fig. 3A), but not the FR ommatidia (Fig. 3B), emit fluorescence under excitation by 420 nm light (Fig. 3A). The fluorescence characteristics appeared to be identical in the two sexes, in contrast with *Pieris rapae* where the female eyes lack fluorescing ommatidia (Arikawa et al., 2005).

After taking the eye shine and fluorescence photographs (Fig. 3A–C), we processed the eyes for light microscopic histology, to see whether the two populations of ommatidia are also histologically different. As expected from our studies on *P. rapae*, we found that the fluorescing/670 nm-reflecting ommatidia have perirhabdomal pigments arranged trapezoidally around the rhabdom

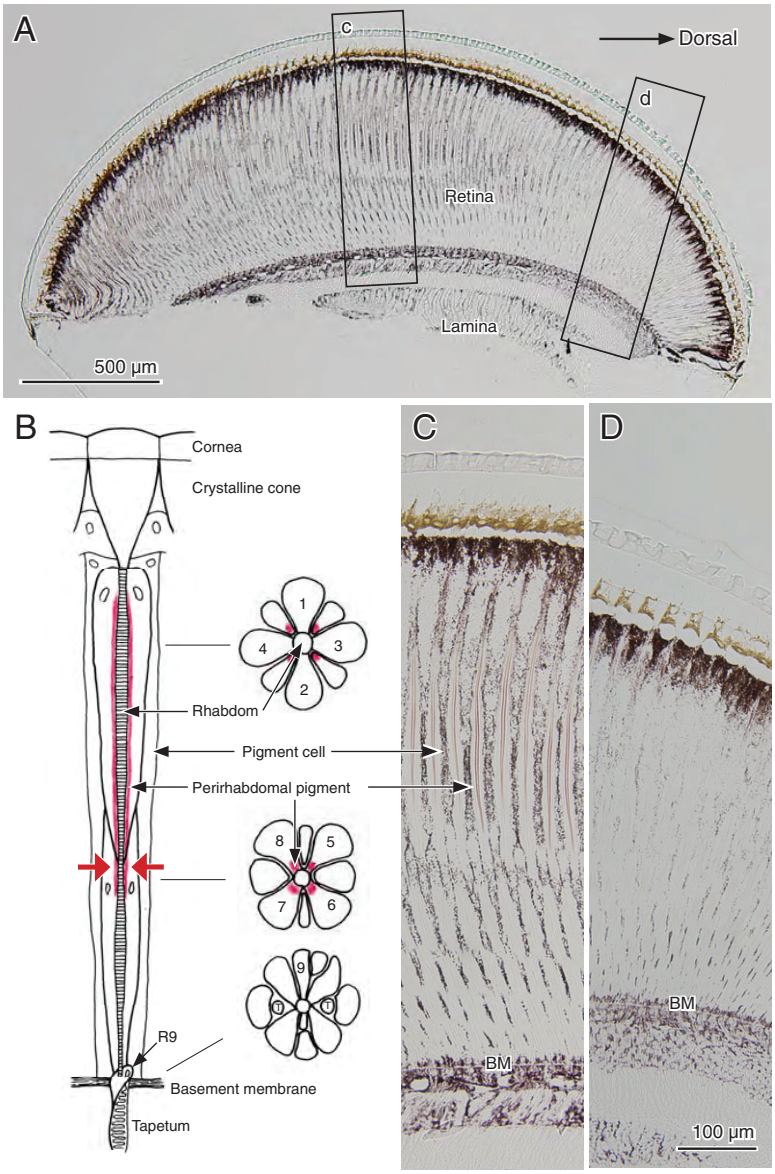

Fig. 1. Compound eye structure of *Colias erate*. (A) Unstained plastic section of a whole compound eye along the ommatidial axis. Right side is dorsal. The boxes (c and d) indicate the areas magnified in C and D. (B) Schematic diagram of a *Colias* ommatidium. Longitudinal (left) and transverse views at three depths (right). 1–9, photoreceptor classes; T, tracheole. Photoreceptors 5–8 contain red perirhabdomal pigment. Red arrows indicate the rhabdom constriction. (C) Longitudinal view of ommatidia in the middle region. (D) Longitudinal view of dorsal ommatidia. BM, basement membrane. Scale bars: 500 µm for A, 100 µm for C and D (shown in D).

(enclosed in the white frames in Fig. 3), while the FR ommatidia have pigment clusters arranged in a square or rectangular pattern (Fig. 3D).

Structural heterogeneity of ommatidia

To describe the ommatidial heterogeneity in detail, we analysed serial sections of the ventral part of an eye with both light and electron microscopy.

Fig. 4 shows a set of pictures of an eye at different depths (Fig. 4A–F). At a depth of 280 µm from the corneal surface, three types of ommatidia are evident (Fig. 4B): here, pigment clusters are arranged in a trapezoidal (type I), square (type II) or rectangular (type III) pattern. Type I contains two subtypes: the shorter side is oriented either dorsally or ventrally. The length of the sides of the trapezoid corresponds to the size of the cell bodies of the R1 and R2 photoreceptors (see Fig. 1B). The cell body on the longer side of the trapezoid is larger than the cell body on the shorter side at the middle level (e.g. Fig. 4C, arrows), but this is reversed at the distal level (Fig. 4A, arrows). Fig. 4G is an electron micrograph at 280 µm depth, showing the same set of ommatidia marked as I, II and III in Fig. 4B, with their diagrammatical sketches below. Type II and III can be distinguished not only by the pigment arrangement but also by the shape of the rhabdom (Fig. 4G).

Although the discrimination of type II and III ommatidia in the light micrographs appeared not to be easy at all depth levels, the shape and size of the rhabdom are nevertheless remarkably different between the three ommatidial types (Figs 5 and 6). Nine photoreceptors contribute their rhabdomeres to form the rhabdom, but not uniformly. For example, at the 280 µm depth level photoreceptors R1–4 bear microvilli in all three ommatidial types (Fig. 5B,E,H), but at 400 µm the rhabdoms of type I, II and III ommatidia are composed of the rhabdomeres of R2–4 (Fig. 5C), R1–8 (Fig. 5F) and R5–8 (Fig. 5I), respectively. To quantify the rhabdom's entire shape, we measured the rhabdom cross-sectional area, and also estimated the relative contribution of each photoreceptor at a given depth on representative electron micrographs. We thus calculated the size of the rhabdomeres along the longitudinal axis of the rhabdom (Fig. 6A–C). The thickest part of the rhabdom is at a depth of 350–400 µm (type I) or 250–350 µm (type II, III); the rhabdom cross-sectional area here is about 8 µm^2.

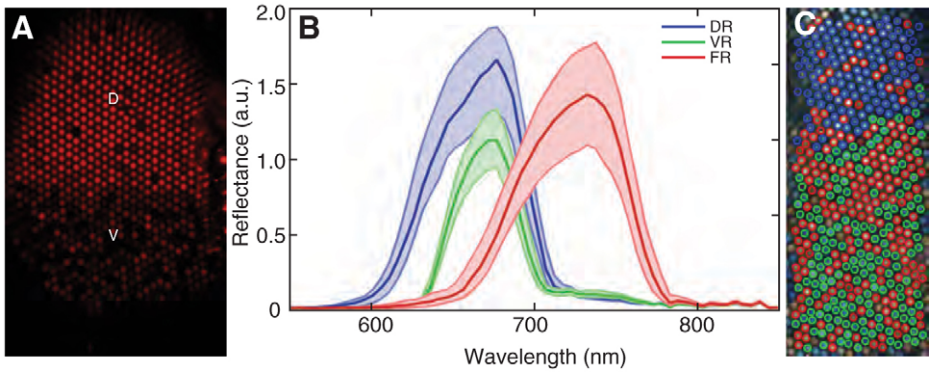

Fig. 2. Imaging microspectrophotometry (IMSP) of tapetal reflections. (A) Tapetal reflection under 660 nm illumination. D, dorsal; V, ventral. (B) Reflectance spectra of the three eye shine types from an IMSP measurement of an individual: dorsal-red (DR, blue, *N*=104), ventral-red (VR, green, *N*=273), far-red (FR, red, *N*=323). Spectra are shown as medians with interquartile ranges. a.u., arbitrary units. (C) Classification of eye shine types based on the reflectance spectra, superimposed on a false-colour image of the eye shine. Colours are the same as in B.

A peculiar feature of the *C. erate* rhabdoms is that they have a constriction (red arrows in Fig. 1B) at a depth of around 500 µm (type I) or 450 µm (type II, III), and they become fatter again proximally. The cross-sectional area of the transitional region is about 1 µm^2 (meaning a very small diameter of *ca*. 0.6 µm; Fig. 6A–C), and the rhabdom is there almost entirely encircled by pigment granules in the cell bodies of R5–8 photoreceptors (Fig. 5I). In the dorsal eye region, we have not found any clear sign of such rhabdom constrictions.

We also quantified the distribution of pigment granules around the rhabdom. There are maximally about 60 spherical granules, with a diameter of 0.1–0.2 µm, as estimated from ultrathin sections (see Fig. 5). The granules are accumulated in the cell bodies of R5–8 photoreceptors in the close vicinity of the rhabdom. The length of the rhabdom part surrounded by the pigment is about 200 µm in all types of ommatidia, with the distribution of pigment slightly displaced proximally in type I ommatidia. The pigment covers the constricted rhabdom region in all types of ommatidia. The region deeper than 550 µm is pigment free (Fig. 6D).

The rhabdomeral microvilli are either straight or curved. In all three ommatidial types, the microvilli deriving from R1–4 photoreceptors curve in two directions. When we define the animals' dorso-ventral axis as 0 deg., which is parallel to the vertical edge of the pictures in Figs 2–5, the R1–4 microvilli curve towards about 45 and 135 deg., suggesting that the polarisation sensitivity of the R1–4 photoreceptors is reduced. On the other hand, the microvilli

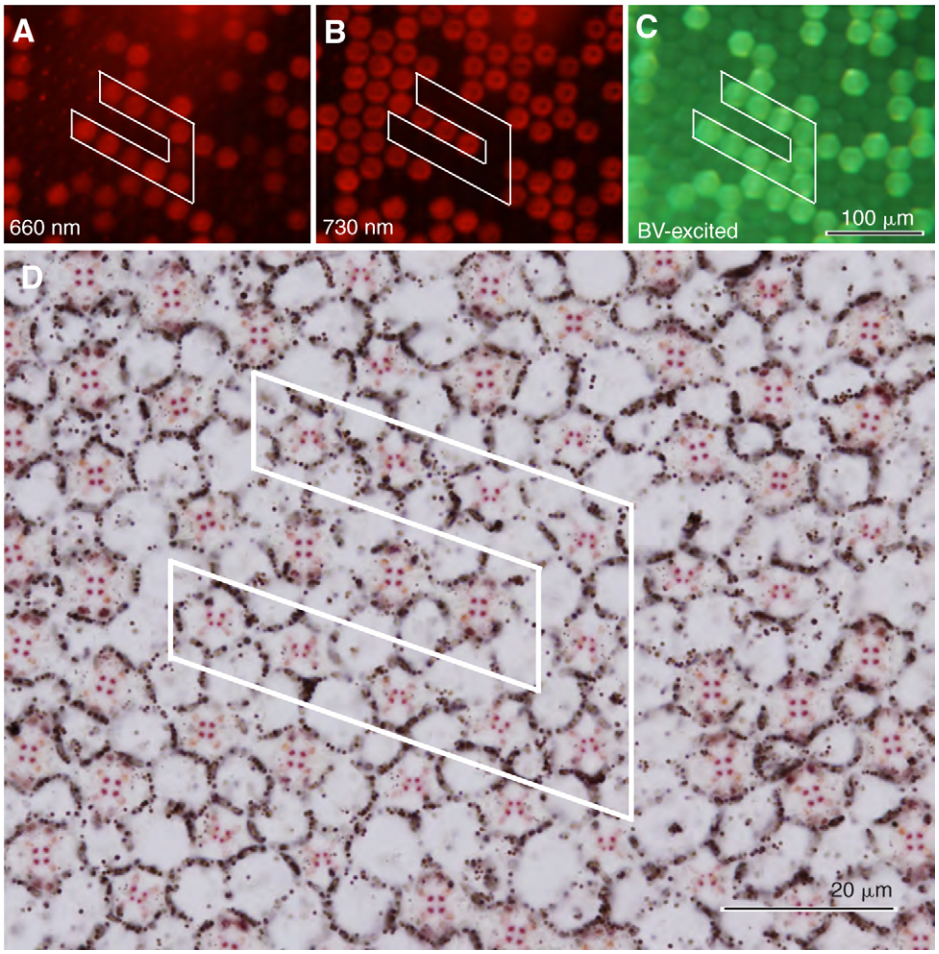

Fig. 3. Tapetal reflection, ommatidial fluorescence and pigmentation. White frames indicate the same set of ommatidia. (A) Tapetal reflection at 660 nm light. (B) Tapetal reflection at 730 nm. (C) Fluorescence under 420 nm epi-illumination. BV-excited, blue–violet excited. (D) Unstained section through the same region of the eye. The fluorescing ommatidia reflect 660 nm and have perirhabdomal pigment clusters trapezoidally arranged around the rhabdom. Scale bars: 100 µm for A–C (shown in C), 20 µm for D.

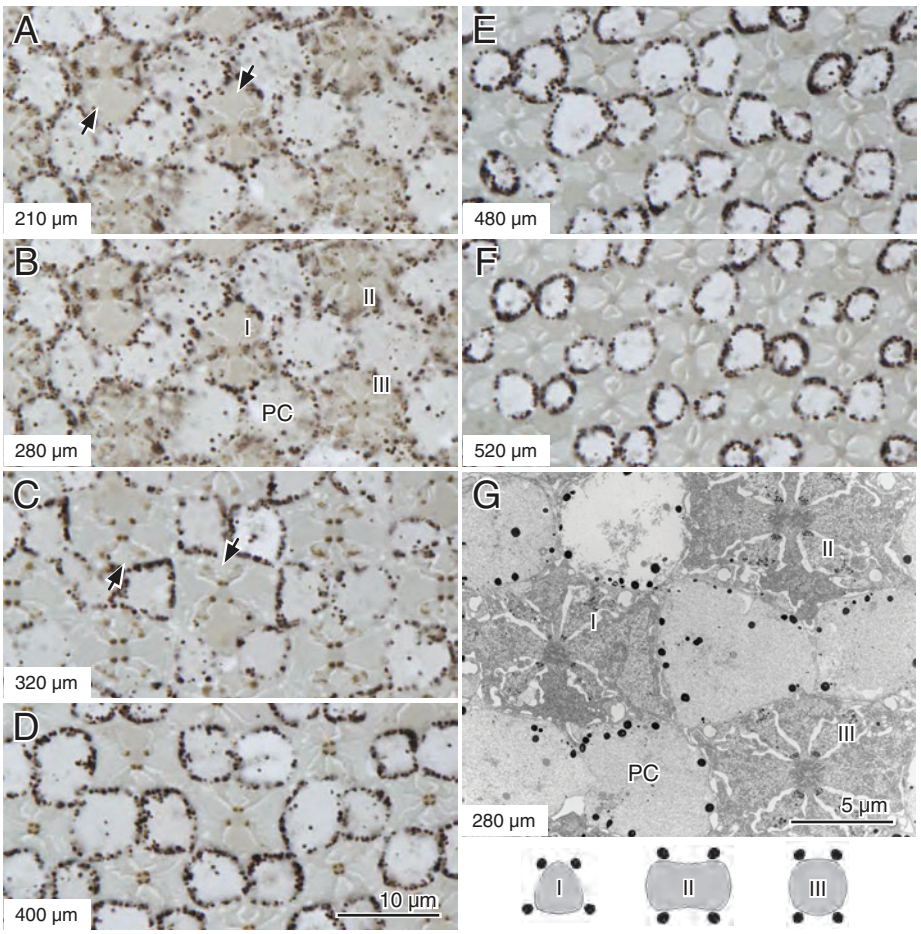

Fig. 4. The same set of ommatidia at six different levels. (A–F) Sections are at 210 µm (A), 280 µm (B), 320 µm (C), 400 µm (D), 480 µm (E) and 520 µm (F) from the corneal surface. (G) Low magnification electron micrograph at 280 µm, showing the three ommatidia marked in B. The three diagrams below indicate a transverse view of the pigment and the rhabdom of the type I, II and III ommatidia. Scale bars: 10 µm for A–F (shown in D), 5 µm for G.

of R5–8 photoreceptors are straight and parallel to the 45 deg. (R5 and R7) or 135 deg. (R6 and R8) directions (Table 1).

Pigment absorption spectra

In transverse sections of the retina, it is easy to identify four reddish pigment clusters surrounding each rhabdom and brown pigment granules in the screening pigment cells between the ommatidia (Fig. 4B,G). We measured the transmittance spectra of the pigment clusters and the surrounding cytoplasm by IMSP in a transverse section at a depth of 330 µm of non-osmicated tissue (Fig. 7). The colour of the perirhabdomal pigment appears to be very similar in all types of ommatidia when visually inspecting the histological sections (Fig. 3D), and indeed the measured transmittance spectra are virtually indistinguishable (Fig. 7).

DISCUSSION

Constricted transitional region of the rhabdom

The fused rhabdom of butterfly eyes is a long and thin cylinder acting as an optical waveguide. Part of the light propagating along a rhabdom travels outside of it as the boundary wave, which is absorbed by pigment surrounding the rhabdom (Land and Osorio, 1990; Stavenga, 2006). The perirhabdomal pigment of *C. erate* has a high transmittance above 600 nm (Fig. 7), so that the pigment acts as a long-pass, short-wavelength-absorbing spectral filter.

Typically, a butterfly rhabdom smoothly tapers from the distal towards its basal end (Gordon, 1977; Kolb, 1977; Kolb, 1985; Qiu et al., 2002). However, the rhabdom of *C. erate* appears to be unique, as it has a severe constriction in the middle of the retinal level (red arrows in Fig. 1B). The rhabdom of *C. erate* proximal to the constriction is made up of rhabdomeres of R5–8 photoreceptors (Fig. 6), or the constriction is located exactly between the distal and the proximal tier. To the best of our knowledge, a similar constriction in the middle of the rhabdom has never been described for any other compound eye.

The fraction of the light flux propagated in the boundary wave increases when the rhabdom diameter decreases (Snyder, 1979). Therefore, in the presence of clusters of pigment lining the rhabdom, the constriction of the rhabdom results in an increased absorption of the light propagating along the rhabdom. In other words, the filtering effect of the pigment clusters is strongly enhanced in the area of the rhabdom constriction. It may be thought that this could be for saving visual pigment production, but a more likely reason is that the constriction functions in a similar way to the intrarhabdomal pigmentation of the midband ommatidia of stomatopod eyes (Marshall et al., 1991). Inevitably, in *C. erate* the rhabdom constriction and the enhanced filtering by the red pigment result in a reduction of the absolute sensitivity of the proximal photoreceptors, but this price is probably paid by achieving a sensitivity peak in the far-red wavelength range. For a diurnal butterfly that is only active in bright light conditions and has 500·µm-long rhabdoms, the reduction in sensitivity is most probably not a serious problem, simply because there is enough light available.

Possible variability of short-wavelength receptors

In addition to the red perirhabdomal pigment, type I ommatidia contain fluorescing pigment (Fig. 3). The pigment fluoresces under

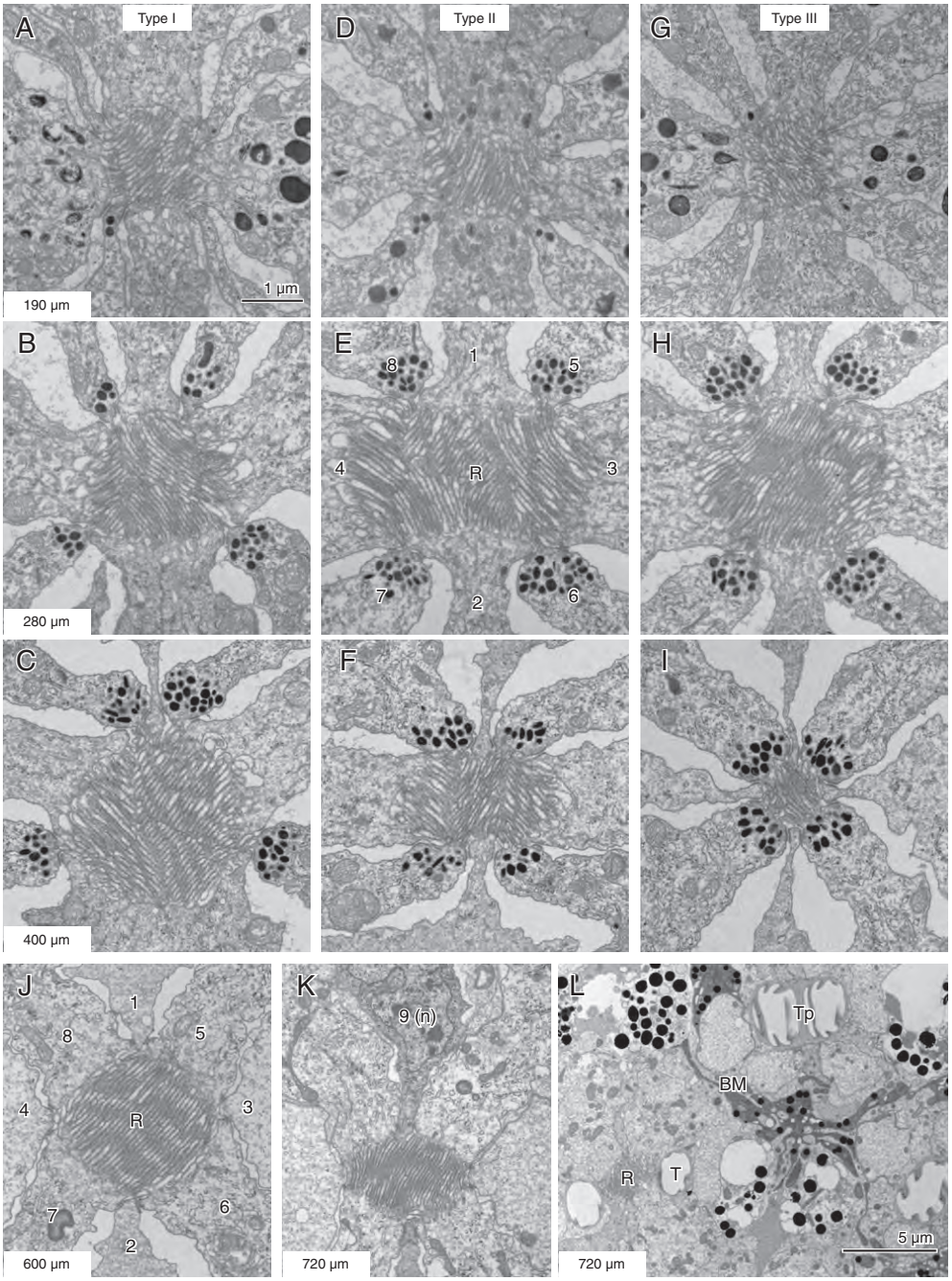

Fig. 5. Transmission electron micrographs of the rhabdoms (R) of the three ommatidial types, I (trapezoidal, A–C), II (square, D–F) and III (rectangular, G–I), at three levels (A,D,G at 190 μm from the corneal surface; B,E,H at 280 μm; C,F,I at 400 μm). (J) Rhabdom at the proximal tier, 600 μm depth. (K) Basal region with R9 at 720 μm depth. (L) Structure around the basement membrane (BM). 1–9, photoreceptor number; n, nucleus; T, tracheole; Tp, tapetum. Scale bars: 1 μm in A–K (shown in A), 5 μm for L.

420 nm excitation light, which is similar to the fluorescence measured in the eyes of *P. rapae* (Qiu et al., 2002) and *Anthocharis scolymus* (Takemura et al., 2007).

Females of *P. rapae* have three short-wavelength receptors, UV, violet (V) and blue (B), each expressing specific visual pigments, PrUV, PrV and PrB, respectively. They are localised either in R1 and or in R2 photoreceptors in three fixed combinations: UV–B, V–V and UV–UV. Males share the expression pattern, but the ommatidia with two PrV-expressing cells also contain a pigment fluorescing under violet light. By acting as a violet filter, the

Table 1. Three types of ommatidia in *Colias erate*

	Ratio	Fluorescence	Reflection	Rhabdomeral microvilli			
				R1–4	R5, 7	R6, 8	R9
I	47%	+	VR 670 nm	Curved, 45 and 135 deg.	Straight, 45 deg.	Straight, 135 deg.	–
II	38%	–	FR 730 nm				
III	14%	–	FR 730 nm				

VR, ventral-red; FR, far-red (see text).

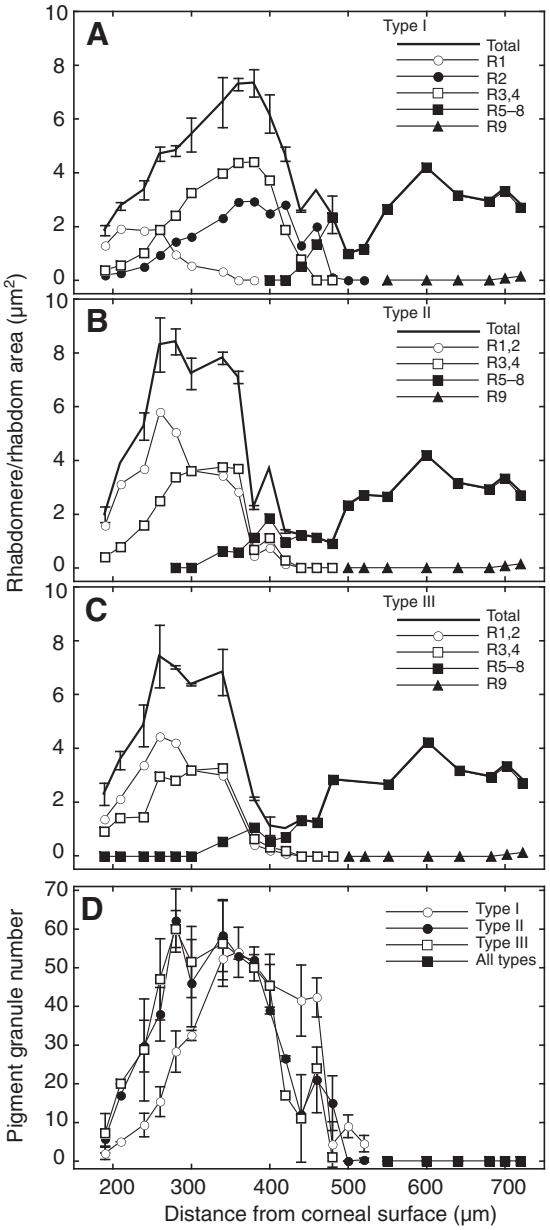

Fig. 6. (A–C) Rhabdom areas (thick line) and rhabdomere areas of R1–9 photoreceptors in type I (A), II (B) and III (C) ommatidia. The rhabdomere areas are rhabdom areas multiplied by rhabdomere fractions at each depth estimated from typical electron micrographs. (D) Distribution of perirhabdomal pigment granules along the longitudinal axis of the ommatidia. Numbers of pigment granules in R5–8 photoreceptors per ommatidium are plotted against the distance from the corneal surface. In the region deeper than 550 μm, ommatidial types could not be discriminated. Data in A–D are means ± s.d.

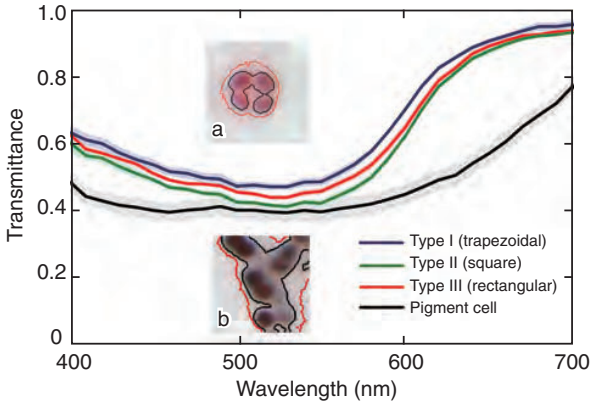

Fig. 7. Transmittance spectra of pigments measured by IMSP. The spectra are means of four type I (blue line), seven type II (green line) and five type III ommatidia (red line, inset a) and 19 brown pigment granules (black line, inset b). The transmittance values of the pigments were estimated directly as an average grey value of the pixels passing the mask area indicated by black lines in the insets, normalised to the average grey value of 11 separately measured non-pigmented areas. The shaded areas represent the standard deviations.

fluorescing pigment turns the V receptors into double-peaked blue (dB) receptors. Male *P. rapae* thus have a set of three short-wavelength receptors, UV, dB and B, which differs from the set of receptors in the female (Arikawa et al., 2005).

The eyes of *P. xuthus* have two short-wavelength-absorbing visual pigments, UV and B type, expressed in R1 and R2 receptors, also in three fixed combinations: UV–B, UV–UV and B–B. The UV–UV type ommatidia also contain 3-OH retinol, which functions as a 320 nm-absorbing spectral filter for the photoreceptors. The screening effect of 3-OH retinol shifts the sensitivity of the UV opsin-bearing photoreceptors to the long wavelength side, making them 400 nm-peaking V receptors (Arikawa et al., 1999a). The PxUV-expressing cells in the non-fluorescing type I ommatidia are UV receptors. Therefore, the eye of *P. xuthus* is also furnished with UV, V and B receptors.

What is the situation in *C. erate*? We recently found that eyes of *C. erate* express three opsins of short-wavelength-absorbing visual pigments in the R1 and R2 photoreceptors (Awata et al., 2009). The opsin expression pattern is, however, quite different from that of *P. rapae*. The short wavelength opsin of *C. erate*, a UV type, is an orthologue of the *Pieris* UV opsin, and two V opsins are both orthologues of the *Pieris* V opsin; we could not find any orthologues of the *Pieris* B opsin. This phylogenetic relationship indicates that at the early stage of evolution of the Pieridae an ancestral B opsin gene duplicated in the common ancestor of the Pierinae and the Coliadinae, eventually forming B and V receptors in *P. rapae*. In the lineage of *Coliadinae*, the ancestral form of the *Pieris* B opsin was lost, yet that of the *Pieris* V opsin independently duplicated. This trait has to be confirmed by comparative studies on other pierid species.

In the retina of *C. erate*, the two V opsins seem to be always expressed together. They are in three fixed combinations in R1 and R2: UV–V1/V2 (type I), V1/V2–V1/V2 (type II), and UV–UV (type III) (Awata et al., 2009). Although the spectral sensitivities of these receptors have yet to be precisely measured, the UV- and V1/V2-bearing photoreceptors are most probably UV and V receptors, respectively. If the fluorescing pigment in the type I ommatidia (Fig. 3) has a function similar to that of *P. rapae*, the 'UV' receptors and 'V' receptors in type I ommatidia are modified by the filtering effect of the fluorescing pigment. The type II and III ommatidia will bear simple V and UV receptors. The richness of short wavelength receptors thus may enhance the wavelength discrimination ability of *C. erate* in the short wavelength range, in a similar way to that in the males of *P. rapae*.

Eye shine and tapetum

The apparent absence of tapetal reflections in the ventral eye region stimulated us to initiate the present study of the *C. erate* eye. It

turned out that the ventral ommatidia do have tapetal reflections. However, because of the strong pigment filters, the reflection is weak and strongly shifted towards the far-red, so that the white light epi-illumination that we used for the initial survey was insufficient to reveal the tapetal reflections. Monochromatic illuminations and long exposure times clearly demonstrated three distinct tapetal reflections, two peaking at 670 nm (DR and VR) and one peaking at 730 nm (FR; Fig. 2).

The tapetal reflection peaking at 730 nm suggests that the FR ommatidia in the eye of *C. erate* eye are sensitive to far-red light. In *P. rapae*, the deep-red tapetal reflection peaks at 675 nm (Qiu et al., 2002). The R5–8 photoreceptors of the type II ommatidia of *P. rapae* are deep-red receptors peaking at 640 nm, while the visual pigment absorbs maximally in the yellow–green wavelength range (absorption peak wavelength 563 nm). The difference between the visual pigment absorption spectrum and the photoreceptor sensitivity spectrum is caused by the red, perirhabdomal pigment filter (Wakakuwa et al., 2004). In type II and III ommatidia of *C. erate*, the reflectance peaks at 730 nm (Figs 2 and 3), having a larger long-wavelength shift than that in *P. rapae*. We recently found that *C. erate*, similar to *P. rapae*, has one long-wavelength-absorbing visual pigment expressed in all R3–8 photoreceptors in all ommatidia (Awata et al., 2009), and we therefore expect that at least part of the R5–8 receptors of *C. erate* will have a red spectral sensitivity with a peak wavelength longer than that of the deep-red receptors of *P. rapae*. In fact, we have repeatedly encountered 660 nm-peaking deep-red receptors in the eye of *C. erate* in preliminary spectral sensitivity measurements with intracellular recordings. In *Pieris brassicae*, red receptors seem to play a role in reproductive behaviour (Scherer and Kolb, 1987) and in *P. xuthus* they are a part of the colour vision system (Koshitaka et al., 2008). In *C. erate*, the function of red receptors has not been elucidated: they may be related to the possible preference for feeding on red flowers (Tanaka, 1991) or to host plant quality assessment.

We thank Dr Norifumi Mogami and Mr Bas Wijnen for technical assistance at an early stage of the work. The work was financially supported by JSPS grants no. 18405008 and 18207004, HCAS/SOKENDAI project grant to K.A., and AFOSR/EOARD grant no. FA8655-08-1-3012 to D.G.S.

REFERENCES

Arikawa, K. and Stavenga, D. G. (1997). Random array of colour filters in the eyes of butterflies. *J. Exp. Biol.* **200**, 2501-2506.

Arikawa, K., Inokuma, K. and Eguchi, E. (1987). Pentachromatic visual system in a butterfly. *Naturwissenschaften* **74**, 297-298.

Arikawa, K., Mizuno, S., Scholten, D. G., Kinoshita, M., Seki, T., Kitamoto, J. and Stavenga, D. G. (1999a). An ultraviolet absorbing pigment causes a narrow-band violet receptor and a single-peaked green receptor in the eye of the butterfly *Papilio*. *Vision Res.* **39**, 1-8.

Arikawa, K., Scholten, D. G. W., Kinoshita, M. and Stavenga, D. G. (1999b). Tuning of photoreceptor spectral sensitivities by red and yellow pigments in the butterfly *Papilio xuthus*. *Zool. Sci.* **16**, 17-24.

Arikawa, K., Wakakuwa, M., Qiu, X., Kurasawa, M. and Stavenga, D. G. (2005). Sexual dimorphism of short wavelength photoreceptors in the small white butterfly, *Pieris rapae crucivora*. *J. Neurosci.* **25**, 5935-5942.

Awata, H., Wakakuwa, M. and Arikawa, K. (2009). Evolution of color vision in pierid butterflies: blue opsin duplication, ommatidial heterogeneity and eye regionalization in *Colias erate*. *J. Comp. Physiol. A Neuroethol. Sens. Neural Behav. Physiol.* **195**, 401-408.

Bernard, G. D. (1979). Red-absorbing visual pigment of butterflies. *Science* **203**, 1125-1127.

Bernard, G. D. and Miller, W. H. (1970). What does antenna engineering have to do with insect eyes? *IEEE Stud. J.* **8**, 2-8.

Briscoe, A. D. (2008). Reconstructing the ancestral butterfly eye: focus on the opsins. *J. Exp. Biol.* **211**, 1805-1813.

Franceschini, N., Kirschfeld, K. and Minke, B. (1981). Fluorescence of photoreceptor cells observed *in vivo*. *Science* **213**, 1264-1267.

Gordon, W. C. (1977). Microvillar orientation in the retina of the nymphalid butterfly. *Z. Naturforsch.* **32c**, 662-664.

Hardie, R. C. (1986). The photoreceptor array of the dipteran retina. *Trends Neurosci.* **9**, 419-423.

Kinoshita, M., Sato, M. and Arikawa, K. (1997). Spectral receptors of nymphalid butterflies. *Naturwissenschaften* **84**, 199-201.

Kolb, G. (1977). The structure of the eye of *Pieris brassicae* L. (Lepidoptera). *Zoomorphology* **87**, 123-146.

Kolb, G. (1985). Ultrastructure and adaptation in the retina of *Aglais urticae* (Lepidoptera). *Zoomorphology* **105**, 90-98.

Koshitaka, H., Kinoshita, M., Vorobyev, M. and Arikawa, K. (2008). Tetrachromacy in a butterfly that has eight varieties of spectral receptors. *Proc. Biol. Sci.* **275**, 947-954.

Land, M. F. and Osorio, D. C. (1990). Waveguide modes and pupil action in the eyes of butterflies. *Proc. Biol. Sci.* **241**, 93-100.

Marshall, N. J., Land, M. F., King, C. A. and Cronin, T. W. (1991). The compound eyes of mantis shrimps (Crustacea, Hoplocarida, Stomatopoda). 2. Colour pigments in the eyes of stomatopod crustaceans: polychromatic vision by serial and lateral filtering. *Philos. Trans. R. Soc. Lond. B Biol. Sci.* **334**, 57-84.

Matic, T. (1983). Electrical inhibition in the retina of the butterfly *Papilio*. I. Four spectral types of photoreceptors. *J. Comp. Physiol. A* **152**, 169-182.

Qiu, X. and Arikawa, K. (2003). Polymorphism of red receptors: sensitivity spectra of proximal photoreceptors in the small white butterfly, *Pieris rapae crucivora*. *J. Exp. Biol.* **206**, 2787-2793.

Qiu, X., Vanhoutte, K. A., Stavenga, D. G. and Arikawa, K. (2002). Ommatidial heterogeneity in the compound eye of the male small white butterfly, *Pieris rapae crucivora*. *Cell. Tissue Res.* **307**, 371-379.

Ribi, W. A. (1978). A unique hymenopteran compound eye: the retina fine structure of the digger wasp *Sphex cognatus* Smith (Hymenoptera, Sphecidae). *Zool. Jb. Anat. Bd.* **100**, 299-342.

Scherer, C. and Kolb, G. (1987). Behavioral experiments on the visual processing of color stimuli in *Pieris brassicae* L. (Lepidoptera). *J. Comp. Physiol. A* **160**, 645-656.

Snyder, A. W. (1979). Physics of vision in compound eyes. In *Handbook of Sensory Physiology*, vol. VII/6A (ed. H. Autrum), pp. 225-313. New York: Springer-Verlag.

Stavenga, D. G. (2002). Reflections on colourful ommatidia of butterfly eyes. *J. Exp. Biol.* **205**, 1077-1085.

Stavenga, D. G. (2006). Invertebrate photoreceptor optics. In *Invertebrate Vision* (ed. E. Warrant and D. E. Nilsson), pp. 1-42. Cambridge: Cambridge University Press.

Stavenga, D. G., Kinoshita, M., Yang, E. C. and Arikawa, K. (2001). Retinal regionalization and heterogeneity of butterfly eyes. *Naturwissenschaften* **88**, 477-481.

Takemura, S. Y., Stavenga, D. G. and Arikawa, K. (2007). Absence of eye shine and tapetum in the heterogeneous eye of *Anthocharis* butterflies (Pieridae). *J. Exp. Biol.* **210**, 3075-3081.

Tanaka, H. (1991). Floral colours preferred by insects. *Insectarium* **28**, 356-360.

Wakakuwa, M., Stavenga, D. G., Kurasawa, M. and Arikawa, K. (2004). A unique visual pigment expressed in green, red and deep-red receptors in the eye of the small white butterfly, *Pieris rapae crucivora*. *J. Exp. Biol.* **207**, 2803-2810.